

# Using the dual approach of FAO-56 for partitioning ET into soil and plant components for olive orchards in a semi-arid region

S. Er-Raki, A. Chehbouni, G. Boulet, D. G. Williams

► **To cite this version:**

S. Er-Raki, A. Chehbouni, G. Boulet, D. G. Williams. Using the dual approach of FAO-56 for partitioning ET into soil and plant components for olive orchards in a semi-arid region. *Agricultural Water Management*, Elsevier Masson, 2010, 97 (11), pp.1769-1778. <10.1016/j.agwat.2010.06.009>. <ird-00667360>

**HAL Id: ird-00667360**

**<http://hal.ird.fr/ird-00667360>**

Submitted on 7 Feb 2012

**HAL** is a multi-disciplinary open access archive for the deposit and dissemination of scientific research documents, whether they are published or not. The documents may come from teaching and research institutions in France or abroad, or from public or private research centers.

L'archive ouverte pluridisciplinaire **HAL**, est destinée au dépôt et à la diffusion de documents scientifiques de niveau recherche, publiés ou non, émanant des établissements d'enseignement et de recherche français ou étrangers, des laboratoires publics ou privés.

1 **Using the dual approach of FAO-56 for partitioning ET into soil and plant**  
2 **components for olive orchards in a semi-arid region**

3  
4 S. Er-Raki<sup>1\*</sup>, A. Chehbouni<sup>2</sup>, G. Boulet<sup>2</sup>, D.G. Williams<sup>3</sup>

5  
6 <sup>1</sup> Cadi Ayyad University / IRD, Marrakech, Morocco

7 Avenue Prince Moulay Abdellah, BP 2390 Marrakech 40000 (Morocco)

8 <sup>2</sup> Centre d'Etudes Spatiales de la Biosphère, Université de Toulouse, CNRS, IRD, CNES, 18

9 Avenue. Edouard Belin, bpi 2801, 31401 Toulouse cedex 9 (France)

10 <sup>3</sup> Departments of Renewable Resources and Botany, University of Wyoming,

11 Laramie, WY 82071, USA

12  
13  
14  
15  
16 \*Corresponding author and current address:

17 Dr. Salah Er-Raki

18 Projet SudMed - Centre Geber salle 26 –Faculty of Science Semlalia,

19 Cadi Ayyad University BP 2390, Marrakech, Morocco

20 Tel. /Fax. (+212) (0) 524 43 16 26

21 Email: [s.erraki@ucam.ac.ma](mailto:s.erraki@ucam.ac.ma)

## 24 **Abstract**

25       The main goal of this research was to evaluate the potential of the dual approach of  
26 **FAO-56 for estimating actual crop evapotranspiration (AET) and its components (crop**  
27 **transpiration and soil evaporation) of an olive (*Olea europaea* L.) orchard in the semi arid**  
28 **region of Tensift-basin (central of Morocco). Two years (2003 and 2004) of continuous**  
29 **measurements of AET with the eddy covariance technique were used to test the performance**  
30 **of the model.** The results showed that, by using the local values of basal crop coefficients, the  
31 approach simulates reasonably well AET over two growing seasons. The Root Mean Square  
32 Error (RMSE) between measured and simulated AET values during 2003 and 2004 were  
33 respectively about 0.54 and 0.71 mm per day. The obtained value of basal crop coefficient  
34 ( $K_{cb}$ ) for the olive orchard was similar in both seasons with an average of 0.54. This value  
35 was lower than that suggested by the FAO-56 (0.62). **Similarly, the single approach of FAO-**  
36 **56 has been tested in the previous work (Er-Raki et al., 2008) over the same study site and it**  
37 **has been shown that this approach also simulates correctly AET when using the local crop**  
38 **coefficient and under no stress conditions.**

39       Since the dual approach predicts separately soil evaporation and plant transpiration, an  
40 attempt was made to compare the simulated components of AET with measurements obtained  
41 through a combination of eddy covariance and scaled-up sap flow measurements. The results  
42 showed that the model gives an acceptable estimate of plant transpiration and soil  
43 evaporation. The associated RMSE of plant transpiration and soil evaporation were 0.59 and  
44 0.73 mm per day, respectively.

45       Additionally, the irrigation efficiency was investigated by comparing the irrigation  
46 scheduling design used by the farmer to those recommended by the FAO model. It was found  
47 that although the amount of irrigation applied by the farmer (800 mm) during the growing  
48 season of olives was twice that recommended one by the FAO model (411 mm), the

49 vegetation suffered from water stress during the summer. Such behaviour can be explained by  
50 inadequate distribution of irrigation. Consequently, the FAO model can be considered as a  
51 potentially useful tool for planning irrigation schedules on an operational basis.

52 **Keywords:** Crop coefficient, Evapotranspiration, Eddy covariance, FAO-56 model, Olea  
53 europaea, Sap flow.

## 54 **1. Introduction**

55           Regions classified as semi-arid or arid constitute roughly one third of the total global  
56 land cover. Within these regions, water scarcity is one of the main factors limiting agricultural  
57 development. The impact of such water scarcity is amplified by inefficient irrigation practices,  
58 especially since the irrigation consumes more than 85% of the available water in these regions  
59 (Chehbouni et al., 2008). Therefore, the first step toward sound management of the scarce  
60 water resources in these regions requires an accurate estimation of the water needs and  
61 consumption of irrigated agriculture. The crop water need is defined as the amount of water  
62 needed to meet the **amount of** water lost to the atmosphere through evapotranspiration.

63           During the last two decades, several models have been developed to simulate crop  
64 evapotranspiration (ET) and in some cases, its components (soil evaporation and plant  
65 transpiration). These models ranged from complex, physically based ones such as the Simple  
66 Soil Plant Atmosphere SiSPAT (Braud et al., 1995), ISBA (Noilhan and Mahfouf, 1996), to  
67 more simple and conceptual ones (Sinclair and Seligman, 1996; Olioso et al., 1999) such as  
68 SVAT simple (Boulet et al., 2000). Other models such as STICS (Brisson, 1998) or CERRES  
69 (Ritchie, 1986) simulate ET through the combination of a water balance with a **crop** growth  
70 component. All of these models need several input parameters which cannot easily be  
71 obtained at the appropriate space-time scale, **and therefore difficult for operational**  
72 **applications.**

73           In addition to the above models/methods, the FAO-56 approach has been extensively  
74 used to derive ET and schedule irrigation on an operational basis. This approach is often  
75 preferred due to its simplicity and its robustness for operational applications. It requires fewer  
76 input data, and provides acceptable ET estimates when compared to heavily parameterized  
77 physically-based models (Evelt et al., 1995; Kite and Droogers, 2000; Eitzinger et al., 2002),  
78 to ground measurement (e.g. Paço et al., 2006; Er-Raki et al., 2007, 2008, 2009; Liu and Luo,

79 2010) or to satellite measurements (e.g. Allen, 2000; Kite and Droogers, 2000; Duchemin et  
80 al., 2006; Er-Raki et al., 2006, 2010). FAO-56 is based on the concepts of reference  
81 evapotranspiration  $ET_0$  and crop coefficients  $K_c$ , which have been introduced to separate the  
82 climatic demand from the plant response (Allen et al., 1998). There are two approaches to  
83 estimate crop evapotranspiration: the single and the dual crop coefficients. The FAO-56 dual  
84 crop coefficient approach (Allen et al., 1998) describes the relationship between maximal  
85 evapotranspiration  $ET_c$  and reference evapotranspiration  $ET_0$  by separating the single  $K_c$   
86 into the basal crop  $K_{cb}$  and soil water evaporation  $K_e$  coefficients, while in the FAO-56  
87 single crop coefficient approach, the effect of both crop transpiration and soil evaporation are  
88 integrated into a single crop coefficient. Many studies have focused on the application of the  
89 single approach for determining olive water requirement within Mediterranean regions (e.g.  
90 Palomo et al., 2002; Abid Karray et al., 2008; Martinez-Cob and Faci, 2010). In semi-arid  
91 Mediterranean region of southern Morocco, Er-Raki et al. (2008) applied also the single  
92 approach over the same study site of this work, and they found that the approach  
93 overestimates AET by about 18% when using the crop coefficient suggested by Allen et al.  
94 (1998). Knowing that the flood irrigation is the most widely used method by the majority of  
95 the farmers in Morocco (as the case of our study site), which accompanied with a large  
96 amount of the water lost through direct soil evaporation (Yunusa et al., 1997), it is worthwhile  
97 to estimate this substantial amount. This can be achieved by partitioning ET into soil and plant  
98 components, which is the main objective of this present study. For the FAO-56 dual crop  
99 coefficient approach, it has been tested for many crops (bean, corn, and sugar beet) at  
100 Kimberly, Idaho (Allen et al., 1996) and tomato and cotton at Fresno, California by Itenfisu  
101 (1998). As reported by Allen (2000), the comparison between estimated and measured ET by  
102 precision weighing lysimeters in all situations gives an error less than 10% for daily ET  
103 estimates. Allen (1999) applied the FAO-56 procedure to a 200,000 ha irrigation project in

104 California to compare the estimated ET with that determined by water balance, and the results  
105 showed that despite the simplicity of the FAO model, estimates of ET were reasonable with a  
106 good accuracy (overestimation of 6%). Allen (2000) also applied his methodology to an  
107 extensive multiple-cropped surface, and compared the estimated ET with one obtained by  
108 remote sensing. Results have shown that the FAO-56 approach overestimated ET by more  
109 than 20%. Recently, several studies used the FAO-56 dual crop coefficient for estimating  
110 water consumptions of different crops (Allen et al., 2005 a, b; Hunsaker et al., 2003, 2005;  
111 Paço et al., 2006; Er-Raki et al., 2007). Some of these studies adopted the FAO-56 dual  
112 approach to use satellite based vegetation index (Hunsaker et al., 2003, 2005; Er-Raki et al.,  
113 2007; González-Dugo and Mateo, 2008; Er-Raki et al., 2010). The results show that relating  
114 the basal crop coefficient  $K_{cb}$  to remotely sensed vegetation index greatly improves the  
115 performance of FAO-56 method. However, Er-Raki et al. (2006) showed that the performance  
116 of the FAO-56 method has some limitations when there is high soil evaporation or when  
117 stress occurs. To overcome this problem and then enhance the FAO-56 performances, ET  
118 derived from thermal infrared (TIR) observations was assimilated into FAO-56 single source  
119 model (Er-Raki et al., 2008) in order to estimate accurately the water consumption of olive  
120 orchards in the semi-arid region of the Tensift basin (central of Morocco).

121 Several studies have been specifically dedicated to estimate ET over olive trees.  
122 Villalobos et al. (2000) determined olive ET by the estimation of its two components, through  
123 a combination of a transpiration model based on the equation of Penmann-Monteith  
124 (Monteith, 1965) and a soil evaporation model similar to that of Ritchie (1972). Palomo et al.  
125 (2002) used a water balance approach, to determine water consumption in olive orchards.  
126 Among the several disadvantages of this approach, summarized by Fernández and Moreno  
127 (1999), is the variability of the hydraulic properties of the soil profile, such as the hydraulic  
128 conductivity-soil water content relationship. Recently, Testi et al. (2004) used the eddy-

129 covariance technique to obtain direct estimates of ET of young irrigated olive orchards in  
130 southern Spain. In the context of SudMed project (Chehbouni et al., 2008), Williams et al.  
131 (2004) used the sap flow method combined with the isotopic method to estimate plant  
132 transpiration and soil evaporation over olive orchards in southern Morocco.

133         Estimating total ET over olive orchards has been investigated by many studies in semi  
134 arid regions (e.g. Fernández et al., 2001; Testi et al., 2004; Ezzahar et al., 2007; Er-Raki et al.,  
135 2008), but there is little information on the partitioning of the relevant components of ET in  
136 such areas; this is one of the most important ecohydrological challenges in understanding  
137 water exchange and vegetation dynamics in arid and semi arid ecosystems (Reynolds et al.,  
138 2000; Huxman et al., 2005). Partitioning ET is possible by using a combination of micro-  
139 meteorological measurements (e.g. Bowen ratio, eddy covariance system), and eco-  
140 physiological techniques (e.g. sap flow, stable isotopes) (Williams et al., 2004; Yepez et al.,  
141 2005; Scott et al., 2006). However, these methods are expensive and difficult to deploy and  
142 maintain in both time and space. Recently, Moran et al. (2009) developed an operational  
143 approach for partitioning ET with a minimal cost and suitable for operation over long time  
144 periods. This approach is based on the difference between the mid-afternoon and pre-dawn  
145 soil surface temperature, which is considered as the indicator of the soil evaporation. In the  
146 same context, the present study aims to use an operational model of FAO-56 dual crop  
147 coefficient approach for partitioning ET. We first compared actual ET derived from this  
148 approach to that measured using an eddy covariance device, then the issue of the ability of  
149 this approach to provide accurate estimates of components of AET through a comparison of  
150 field data obtained from a combination of eddy covariance based AET measurements and  
151 spatialized or scaled-up sap flow measurements of transpiration. In this context the objectives  
152 of this study were:



- 153 1. to analyze the ability of the FAO-56 dual crop coefficient model to reproduce the  
154 temporal evolution of evapotranspiration and its components: plant transpiration  
155 and soil evaporation. Actual plant transpiration was compared with scaled-up sap  
156 flow measurements.
- 157 2. to estimate the most adequate water quantity needed for the olive and to determine  
158 the best timing of irrigation by using the FAO-dual approach.

159 This paper is organized as follows. Section 2 presents a description of study site and  
160 data collected during the 2003 and 2004 growing season. In Section 3, we provide a brief  
161 theoretical overview of the FAO-56 dual crop coefficient approach. Section 4 presents an  
162 application of this approach over an olive site. Also in this section, we analyze the ability of  
163 this approach to reproduce the temporal evolution of both components of evapotranspiration  
164 (plant transpiration and soil evaporation), and to derive the soil water stress coefficient  $K_s$  of  
165 olives orchards during growing season in order to determine the best timing of irrigation. In  
166 the final section, summary and conclusion are provided.

## 167 **2. Experimental Data**

168 The experimental data used for this research are similar to those used in the previous  
169 paper (Er-Raki et al., 2008). Here, we presented briefly the site description, climatic and eddy  
170 covariance measurements. However, as the main objective of this work is the partitioning of  
171 actual evapotranspiration (AET) into plant transpiration and soil evaporation through a  
172 combination of eddy covariance and scaled-up sap flow measurements, more detailed  
173 presentation of sap flow measurements and its scaled-up to stand level transpiration, which is  
174 not used in a previous paper (Er-Raki et al., 2008), is required.

### 175 **2.1. Site description**

176 This study was carried out during 2003 and 2004, in the Agdal olive (*Olea europaea* L.)  
177 orchard located in the semi-arid region of the Tensift basin, south-east of Marrakech,

178 Morocco (31.601 N, 7.974 W). This area has a mean total annual precipitation of 240mm and  
179 a corresponding mean annual reference evapotranspiration of 1600 mm. The average annual  
180 temperature is about 22°C, rising to 38 °C in the summer (July-August) and going down to 5  
181 °C in winter (December-January). Mean seasonal wind speed was about 1.2 m/s. The  
182 experimental field is almost flat, planted with 240-year old olive trees, grown in an orchard of  
183 about 275 ha. The density of olive trees was about 225 trees per hectare, which provides an  
184 area of about 45 m<sup>2</sup> occupied by each tree. The soil type is homogeneous, with silt clay loamy  
185 texture (30% clay, 25% silt, and 44% sand). The groundwater depth is approximately 40 m.  
186 The soil surface was partly covered ( $\approx$  20%) by natural grass (under story) consisting mainly  
187 of short weeds during most of the year. More details about the site description are given in  
188 Williams et al. (2004) and Er-Raki et al. (2008).

## 189 ***2.2. Data description***

### 190 ***2.2.1. Meteorological data and eddy covariance measurements***

191 All climatic parameters (solar radiation, air temperature, relative humidity and wind  
192 speed), needed for estimate daily reference evapotranspiration ( $ET_0$ ) by the FAO-Penman  
193 Monteith (Equation 6 in FAO-56, Allen et al., 1998) are measured. More details about the  
194 instruments (type, position) used for measurements of these parameters collected over our  
195 study site are provided in Er-Raki et al. (2008).

196 Figure 1 reports the daily pattern of  $ET_0$  calculated by the FAO-Penman-Monteith  
197 equation for the two olive growing seasons (2003 and 2004). The temporal evolution of  $ET_0$   
198 during the year is typically that of a semi-arid continental climate. It is characterised by a high  
199 climatic demand, with the lowest during rainy periods (winter) and the highest values  
200 occurred in the sunny days (summer). Precipitation temporal patterns over the growing season  
201 of olive trees were characterized by low and irregular rainfall events, with a total precipitation  
202 amount of about 280 mm (Figure 1). The amount and timing of irrigations applied by the

203 farmer are presented also in this figure. It was about 800 mm for each season (2003 and 2004)  
204 of olives with around 100 mm in each supply. This irrigation scheme used by the farmer has  
205 been evaluated in this study.

206 **In addition to climatic measurements, an eddy covariance system, constituted with a**  
207 **3D sonic anemometer (CSAT3, Campbell Scientific Ltd.) and an open-path infrared gas**  
208 **analyzer (Li7500, Licor Inc.), was installed over olive tree to provide continuous**  
209 **measurements of vertical fluxes of heat and water vapour at 9.2 m. A detailed description of**  
210 **eddy covariance measurements can be found in Ezzahar et al. (2007) and Er-Raki et al.**  
211 **(2008). As reported also in the same papers, the approximate fetch (spatial scale) of**  
212 **evapotranspiration measurement is about 40m in the** northwestern direction. It might be  
213 considered adequate as it contributed 90% of the measured sensible heat flux (Hoedjes et al.,  
214 2007) and it includes the trees where the sap flow measurements were taken. Data sets of  
215 latent heat and sensible heat fluxes have been available during 2003 and 2004 growing  
216 seasons of olive orchards. Missing data in some days is associated to the collapse of power  
217 supply.

218 **The evaluation of the flux measurements is undertaken through the analyzing the**  
219 **energy balance closure. By ignoring the term of canopy heat storage and the radiative energy**  
220 **used in photosynthesis (Testi et al., 2004; Baldocchi et al., 2000), the energy balance closure**  
221 **is defined as:**

$$222 \quad R_n - G = H_{EC} + L_v E_{EC} \quad (1)$$

223 Where  $R_n$  is the net radiation;  $G$  is the soil heat flux;  $H_{EC}$  and  $L_v E_{EC}$  are respectively  
224 the sensible heat flux and the latent heat flux measured by eddy covariance system. Figure 2  
225 shows how well the available energy ( $R_n - G$ ) was balanced by ( $H_{EC} + L_v E_{EC}$ ) at daily time  
226 scale for the 2003 and 2004 growing season of olive orchards. The slope of the regression  
227 forced through the origin was 1.06 in 2003 and 1.07 in 2004, indicating an underestimation of

228 the flux ( $H_{EC} + L_v E_{EC}$ ) was less than 10% of the available energy ( $R_n - G$ ), with the Root  
229 Mean Square Error (RMSE) being about  $17 \text{ w.m}^{-2}$  in 2003 and  $19 \text{ w.m}^{-2}$  in 2004 (the equation  
230 used to calculate *RMSE* is presented in Appendix). These results indicate --at least at the daily  
231 time scale-- a good closure of the energy balance, which is in agreement with other studies  
232 (Testi et al., 2004; Baldocchi et al., 2000; Twine et al., 2000).

### 233 **2.2.2. Sap flow measurements**

234 Heat-pulse sap flow sensors (Heat Ratio Method, HRM, Burgess et al., 2001) were used to  
235 measure xylem sap flux on eight olive trees. The HRM method has been described in detail in  
236 Burgess et al. (1998) and Burgess et al. (2001). Briefly, the HRM is a modification of the  
237 Heat Pulse Method (HPM) and it employs temperature probes inserted into the active xylem  
238 at equal distances down- and upstream from a heat source. This method improves on the HPM  
239 by its precision at very slow flow rates and even reverses sap flow can be measured.  
240 Reliability of this technique for determining transpiration has been demonstrated by several  
241 studies (Burgess et al., 2001; Fernández et al., 2001 and Williams et al., 2004). The heat pulse  
242 sensors were installed on four large single-stemmed and on four large multi-stemmed trees  
243 adjacent to the eddy covariance tower during the summer of 2003 and 2004. Sap flow  
244 measurements were conducted from the 14<sup>th</sup> of June (DOY 165) through the 30<sup>th</sup> of July  
245 (DOY 211) during 2003 and from the 9<sup>th</sup> of May (DOY 130) through the 28<sup>th</sup> of September  
246 (DOY 272) during 2004. Missing data in some days (from DOY 183 to DOY 194 and from  
247 DOY 222 to DOY 224) is due to problems with the power supply. The same measurements of  
248 sap flow, with the same sensors and over the same field have been made by Williams et al.  
249 (2004) except in other climatic conditions (during the winter). A detailed description of HRM  
250 technique and the principle of measurements can be found in Williams et al. (2004).  
251 Volumetric sap flow ( $\text{L day}^{-1}$ ) was scaled to tree transpiration ( $\text{mm day}^{-1}$ ) using a survey of  
252 the average ground area of each tree ( $45 \text{ m}^2$ ). After the scaling the measured sap flow to the

253 single tree transpiration, we extrapolated this latter to the stand level transpiration, which is  
254 representative for the whole field. The allometric method is the most one used for this up  
255 scaling (e.g. Kumagai et al., 2005; Ford et al., 2007). However, this method is destructive and  
256 very time-consuming. Nevertheless, in this study the extrapolation of the tree transpiration to  
257 the stand level transpiration has been performed based on the measurements of eddy  
258 covariance. This strategy was also proposed by Williams et al. (2004) and Oishi et al. (2008)  
259 in the context of scaling ecosystem-level transpiration from sap flux measurements based on  
260 the measured AET by eddy covariance system. In the same context, we tried to find the  
261 relationship between the scaled measured sap flow and measured AET by eddy covariance,  
262 equivalent to tree level transpiration, during the dry conditions (when the soil evaporation is  
263 negligible). In order to select the dry period, daily evolution of  $\Delta\theta$  was plotted from DOY 195  
264 to DOY 219 (Figure 3), when  $\Delta\theta$  means the difference between the soil moisture at 5 cm  
265 depth on day i and on day i-1. One assumes that  $\Delta\theta$  is proportional to the soil evaporation flux  
266 at least several days after a major irrigation, i.e. when the excess water has been redistributed  
267 within the soil moisture profile. By analysing this figure, one can see that  $\Delta\theta$  increased in  
268 absolute value from DOY 195 to DOY 202, and after it decreased until DOY 212. After this  
269 day,  $\Delta\theta$  is almost constant and close to zero. Therefore, the soil moisture ( $0.13 \text{ m}^3/\text{m}^3$ )  
270 correspond to DOY 212 was considered as the threshold which can be the indicator of the  
271 presence of soil evaporation. When the soil moisture at 5 cm is lower than this threshold, the  
272 soil evaporation is considered negligible regarding the large values of  $ET_0$  during the  
273 summer. After the selection of the dry conditions, measured daily AET by eddy covariance  
274 system was plotted against the daily scaled sap flow measurements (data not presented here).  
275 Then, the obtained linear regression between daily stand level transpiration and daily scaled  
276 sap flow is:

277 Stand level transpiration=  $1.25 * (\text{scaled sap flow})$ ,  $R^2=0.74$  (2)

278 This model was applied also for the remaining days (wetting days) of sap flow  
279 measurements for calculating the stand level transpiration. This may create some errors in  
280 estimating stand level transpiration as reported by Oishi et al. (2008) when they found that the  
281 agreement between the estimates of components AET is greatly affected by the scaling  
282 procedure.

### 283 3. Theoretical overview of the FAO-56 dual approach

284 Detailed descriptions of the FAO-56 dual crop coefficient approach are available from  
285 Allen et al. (1998). In this section, we will briefly present this approach. The actual crop  
286 evapotranspiration (AET) estimated by this approach is given by the following equation:

$$287 \quad AET = (K_s K_{cb} + K_e) ET_0 \quad (3)$$

288 Where  $K_{cb}$ ,  $K_e$  and  $K_s$  are basal crop coefficient, soil evaporation and water stress  
289 coefficient, respectively. The required equations for deriving these three parameters are  
290 presented henceforth.

#### 291 3.1. Calculation of $K_{cb}$

292 The methodology adopted here to compute basal crop coefficient ( $K_{cb}$ ) follows  
293 strictly the same method displayed in Er-Raki et al. (2008) for calculating crop coefficient  
294 ( $K_c$ ). As mentioned previously in the introduction, two different crops (olives and under  
295 story) grew up together in the same field. A simple formula was used to calculate the  
296 equivalent basal crop coefficient (Allen et al., 1998):

$$297 \quad K_{cbfield} = f_{c-olives} K_{cbngc} + (1 - f_{c-olives}) K_{cbcov er} \quad (4)$$

298 Where  $K_{cbngc}$  and  $K_{cbcov er}$  are basal crop coefficients for olive and under story,  
299 respectively. The average seasonal value of basal crop coefficient of olive orchards ( $K_{cbngc}$ )  
300 was derived based on sap flow measurements. For the basal crop coefficient of under story

301 ( $K_{cb\ cover}$ ), it was assumed equal to the difference between the ratio of measured  $AET$  and  $ET_0$

302 ( $K_c = \frac{AET}{ET_0}$ ) and  $K_{cbngc}$  during the dry conditions.  $f_{c-olives}$  is the fraction of soil surface

303 covered by olive trees, calculated as  $f_{c-olives} = \frac{\pi D^2 N}{40000}$  where  $D$  (m) is the average diameter of

304 the canopy and  $N$  is the number of trees per hectare. It was found to be equal to about 0.60.

### 305 **3.2. Calculation of $K_e$**

306 This coefficient is calculated based on daily computation of the water balance for the

307 surface soil evaporation layer  $Z_e$  (equation 71 in FAO-56 paper). The calculation procedure

308 requires input of soil parameters such as the soil moisture at field capacity ( $\theta_{fc}$ ) and at the

309 wilting point ( $\theta_{wp}$ ), the total evaporable water ( $TEW$ ), the readily evaporable water ( $REW$ )

310 and the depth of  $Z_e$ . An average value of  $0.32\ m^3\ m^{-3}$  for  $\theta_{fc}$  and  $0.19\ m^3\ m^{-3}$  for  $\theta_{wp}$  were

311 obtained (Er-Raki et al., 2008). For the depth of the soil surface evaporation layer  $Z_e$  (m),

312 Allen et al. (1998) suggested values ranging between 0.10 and 0.15 m. Because the soil is

313 covered with herbs and is shaded by trees, the value of  $Z_e = 0.15\ m$  is adopted in this study. A

314 typical  $REW$  value for a silt clay loamy soil of 9 mm (FAO-56, table19) was used in the

315 calculations. Another parameter is needed for the calculation of  $K_e$ . This parameter is named

316 the exposed and wetted soil fraction ( $f_{ew}$ ). It was derived following the suggestions of Allen

317 et al. (1998) (equation 75 in FAO-56 paper). In fact, following irrigation (flooding technique)

318 or rainfall, the soil was completely wetted except the area covered by the stem ground tree.

319 This area represents about 5% of the whole area occupied by each tree. Then, the fraction of

320 soil surface wetted by irrigation or precipitation  $f_w$  was about 0.95 and  $f_{ew}$  was equal to  $(1-$

321  $f_c)$ . In the absence of the rainfall and irrigation, it was equal to  $f_w \cdot f_c$ .  $f_c$  represents the fraction

322 of soil surface covered by olive trees and understory, which it was set at 0.80.

### 323 3.3. Derivation of $K_s$

324 When the dual crop coefficient approach is adapted, the effects of soil water stress on  
325 crop  $AET$  are accounted by multiplying the basal crop coefficient by the water stress  
326 coefficient,  $K_s$ . Mean water content of the root zone is expressed by the root zone depletion,  
327  $D_r$ . At field capacity, the root zone depletion is zero ( $D_r = 0$ ). Water stress occurs when  $D_r$   
328 becomes greater than  $RAW$ , the depth of readily available water in the root zone. For  $D_r >$   
329  $RAW$ ,  $K_s$  is given by:

$$330 K_s = \frac{TAW - D_r}{TAW - RAW} = \frac{TAW - D_r}{(1-p)TAW} \quad (5)$$

331 Where  $K_s$  is a dimensionless transpiration reduction factor dependent on available  
332 soil water [0–1],  $D_r$  is root zone depletion [mm],  $TAW$  is total available soil water in the root  
333 zone [mm], and  $p$  is the fraction of  $TAW$  that a crop can extract from the root zone without  
334 suffering water stress. When  $D_r \leq RAW$ ;  $K_s = 1$ .

335  $TAW$  is estimated as the difference between the water content at field capacity and  
336 wilting point:

$$337 TAW = 1000 \left( \theta_{fc} - \theta_{wp} \right) Z_r \quad (6)$$

338 Where  $Z_r$  is the effective rooting depth [m].

339 Readily available soil water of the root zone is estimated as:

$$340 RAW = pTAW \quad (7)$$

341 The required soil parameters for calculation of  $K_s$  are taken from Er-Raki et al.  
342 (2008).  $TAW$  and  $RAW$  values calculated from equation (6) and (7) are 208 and 135.2 mm,  
343 respectively. The rooting depth  $Z_r$  of olive trees and the depletion fraction  $p$  were set at 1.60  
344 m and 0.65 respectively, according to FAO-56 values (table 22).



## 345 **4. Results and discussions**

### 346 ***4.1. Estimating AET by the FAO-56 dual crop coefficient approach***

347 **We calculated the variation over time of** actual evapotranspiration (AET) using the  
348 FAO-56 dual crop coefficient approach over olive trees during two consecutive growing  
349 seasons (2003 and 2004). The simulation was performed from March, 1<sup>st</sup> (DOY 60) to  
350 November, 25<sup>th</sup> (DOY 329) for 2003, and from the March, 1<sup>st</sup> (DOY 61) to November, 7<sup>th</sup>  
351 (DOY 312) for 2004. The average seasonal value of basal crop coefficient of olive orchards  
352 used for the simulation was about 0.54. This value was derived based on sap flow  
353 measurements during 2003. It was expressed as the ratio of measured transpiration by sap  
354 flow to the reference evapotranspiration  $ET_0$ . When sap flow measurements are not available,  
355 basal crop coefficient has been derived based on minimum values of measured crop  
356 coefficient (ratio of measured AET to  $ET_0$ ) according to Teixeira et al. (2008). The  
357 comparison between measured and predicted AET (figure 4) shows good agreement between  
358 observed and simulated AET values. The Root Mean Square Error (RMSE) between  
359 measured and simulated AET values during 2003 and 2004 were respectively about 0.54 and  
360 0.71 mm per day. **Some discrepancies between measured and simulated AET can be clearly**  
361 **observed around wetting events (irrigation and rainfall) and stress period. For wetting events,**  
362 **the difference between measured and simulated AET values may be due to the deep**  
363 **percolation and the rainfall interception, which not taken into account by the model. As**  
364 **reported by Gomez et al. (2001), rainfall interception plays an important component of the**  
365 **water balance, and they showed that the water intercepted by the rainfed olive orchards was**  
366 **about 8% for a heavy rainfall. Another factor that may partly explain some of the difference**  
367 **between measured and simulated AET values is the flux source area measured by eddy**  
368 **covariance which depends to the wind direction. In fact, the eddy covariance system measures**  
369 **the evapotranspiration over a relatively large area (wet and dry) whereas the model simulates**

370 it locally (wet or dry). Moreover, the dual approach tends to overestimate the crop  
371 evapotranspiration at the peak values (wetting events). This is corroborated by Liu and Luo  
372 (2010) when they found that the dual approach of FAO-56 is appropriate for simulating the  
373 total quantity of evapotranspiration but inaccuracy in simulating the peak value after  
374 precipitation or irrigation (Peng et al., 2007). This necessitates a more profound study for  
375 improving some parameterisation used in the FAO-56 method. For the periods of hydric stress  
376 (ex. from DOY 212 to DOY 238 during 2004), the approach leads to higher values of AET in  
377 comparison with that measured by the eddy covariance system. This may be due to an  
378 overestimation of soil water stress coefficient. The overestimation of soil water stress can be  
379 related to the overestimation of the rooting depth (1.6 m). This misrepresentation of the  
380 rooting depth influences directly the ability of the plant to extract water. A similar result has  
381 been found when using the single approach for estimating water consumption for the same  
382 olive orchard (Er-Raki et al., 2008). To illustrate more clearly the effect of the rooting depth  
383 ( $Z_r$ ) on evapotranspiration, it is essential to perform a sensitivity analysis of the FAO model to  
384 this parameter. The impact of rooting depth on AET (data not shown here) showed that the  
385 values of simulated AET increase with increasing of  $Z_r$ . In fact, an increase in  $Z_r$  causes an  
386 increase of Total Available Water (TAW) within the root zone and leads to an increase in the  
387 soil water stress coefficient  $K_s$  which is straightforward according to the equations (6) and  
388 (7). An increase in  $Z_r$  of 33.33%, 66.66%, and 166% (from 1.2 to 1.6, from 1.2 to 2 from 1.2  
389 to 3.2 m, respectively) leads to an increase of AET by about 34%, 47% and 49%, respectively.  
390 Note that the effect of rooting depth on AET is negligible when the water is not limiting  
391 within the root zone.

392 According to this study, the FAO-56 dual crop coefficient approach simulates  
393 reasonably well the total evapotranspiration. The question addressed after is how efficiently

394 this approach simulates the two components individually: plant transpiration and soil  
395 evaporation.

396

#### 397 ***4.2. Performance of the dual crop coefficient approach for Partitioning of*** 398 ***evaporation and transpiration***

399 The FAO-56 dual crop coefficient approach computes separately soil evaporation and  
400 plant transpiration; it is of interest to investigate how well these individual components are  
401 simulated. To achieve this objective, we combined eddy covariance based measurement of  
402 AET with scaled-up sap flow measurements to estimate soil evaporation and plant  
403 transpiration against which the simulated components will be compared. As stated above, sap  
404 flow measurements were conducted from DOY 130 to DOY 272 during 2004. The sum of  
405 measured soil evaporation and the under story transpiration was computed as the difference  
406 between AET measured by the eddy covariance and the olive transpiration measured by the  
407 sap flow method. For practical reasons, the heat pulse sensors were inserted only into the  
408 active xylem of olive trees. Therefore, we compared the simulated soil evaporation with the  
409 sum of measured soil evaporation and the under story transpiration. Also, because the FAO-  
410 dual approach predicts separately only soil evaporation and plant transpiration (olives + under  
411 story) and does not discriminate between the three components (soil evaporation, olive  
412 transpiration and under story transpiration), we compared the simulated plant transpiration  
413 with the measured olive transpiration only.

414 Figure 5a presents a comparison between the measured and simulated transpiration for  
415 the 2004 growing season. Daily patterns are very similar and respond to that of  $ET_0$  (see  
416 Figure1-bottom). The RMSE between measured and simulated olive transpiration was about  
417 0.59 mm per day. The cumulated values of the entire experimental period (128 days) are 362  
418 mm for the transpiration measured by the HRM method and 387 mm for the model, leading to

419 a difference of 7%. This difference is consistent with the fact that the model simulates the  
420 olive transpiration and the under story transpiration while the measurement estimates only the  
421 olive transpiration. Another factor that may partly explain this difference is that the scaling  
422 approach (Eq. 2) is not error-free (Fernández et al., 2001; Williams et al., 2004).

423         Regarding soil evaporation, Figure 5b shows that in dry conditions (absence of  
424 irrigation and rainfall) both simulated and measured soil evaporation are almost zero. It  
425 should be noted that the observed negative values of measured soil evaporation are considered  
426 as an artefact and set to zero. After irrigation or rainfall, as expected, both measured and  
427 estimated soil evaporation increased. However the increasing magnitude is different. This  
428 error is likely due to the fact that:

429             1) the model simulate only soil evaporation, but the measurement gives the soil  
430 evaporation and under story transpiration;

431             2) the scaling approach of measured transpiration from the eddy covariance (Eq. 2)  
432 may not be valid in humid conditions and tends to underestimate the measured plant  
433 transpiration and thus overestimate soil evaporation, also this error can be related also to the  
434 under story contribution;

435             3) the impact of the difference in the footprint of the eddy covariance and the area  
436 where the measured sap flow was taken during the irrigation events. This may be  
437 underestimates or overestimates measured evaporation.

438         Despite those discrepancies between the measured and simulated soil evaporation, the  
439 model gives acceptable results in estimating soil evaporation. The RMSE between simulated  
440 and measured soil evaporation (+ under story transpiration) was 0.73 mm per day.

441         The ratio of plant transpiration and soil evaporation to total evapotranspiration (data  
442 not shown here) showed that before irrigation, plant transpiration represents 100% of total  
443 evapotranspiration and decrease to about 65% after irrigation. An amount of 35% of water

444 was lost by direct soil evaporation due to flooding irrigation and the olive trees are widely  
445 spaced. Another study was done over the same field by Williams et al. (2003, 2004) in winter.  
446 It showed that after the irrigation, the soil evaporation represents about 14–28% of the total  
447 evapotranspiration. Yunusa et al. (1997) also studied the partitioning of seasonal  
448 evapotranspiration from a commercial furrow-irrigated Sultana vineyard, and they found that  
449 substantial amounts of the soil water (about 49% of total ET) were lost through soil  
450 evaporation. In order to prevent the water losses by evaporation from the ground, it is very  
451 important to wet the maximum volume of root zone and the minimum soil surface. Therefore,  
452 a localized irrigation system is usually the most appropriate.

453 Despite the simplicity of the water balance model used in the FAO-56 formulation, the  
454 obtained results showed that the FAO-56 dual crop coefficient can simulate correctly crop  
455 evapotranspiration and gives also an encouraging result for partitioning of evapotranspiration  
456 into soil evaporation and plant transpiration. Because this approach is very simple and  
457 designed to schedule irrigation on an operational basis, it is of interest to check the irrigation  
458 planning practiced by the farmer over the study site. This can be achieved by applying the  
459 FAO model in order to determine when to irrigate and how much water to apply.

460

### 461 ***4.3. Assessment of irrigation planning***

462 In order to assess the efficiency of the irrigation planning over the study site, we  
463 calculated the soil water stress coefficient  $K_s$  by the FAO-56 dual approach (Figure 6a). The  
464 soil water stress coefficient,  $K_s$ , for olive orchards ranges from 0 to 1 according to Equation  
465 (5), and it shows how the soil water depletion,  $D_r$ , changes to limit crop evapotranspiration.  
466 The value of  $K_s$  depends on the soil water depletion linked to water supply (rainfall or  
467 irrigation). The soil water stress is equal to 1 when the soil water depletion is less than the  
468 readily available water of the root zone (*RAW*). The absence of irrigation and rainfall (from

469 DOY 191 to DOY 237) results in an increase in the root zone depletion that exceeds *RAW* and  
470 generates stress ( $K_s$  below to 1). The increase in soil water depletion is due to the removal of  
471 water by evapotranspiration and percolation losses that induces water stress conditions. The  
472 information obtained from the soil water stress coefficient can be used in an irrigation  
473 scheduling program for deciding when and how much to irrigate. For this purpose, we used  
474 the FAO-56 dual approach to simulate the amount and the frequency of irrigation needed  
475 (figure 6a) for olive orchards in 2004 to avoid water stress (i.e. so that  $K_s=1$  at all times).  
476 Following the FAO-56 procedure, irrigation is required when rainfall is insufficient to  
477 compensate the water lost by evapotranspiration. By calculating the soil water balance of the  
478 root zone on a daily basis (Equation 85 in FAO-56), the timing and the depth of the irrigations  
479 can be planned (Figure 6a). According to this figure, the average amount of irrigation in each  
480 supply was about 136 mm which corresponds to the value of *RAW*. The total irrigation  
481 recommended by the model was about 411 mm which it is half that given by the farmer (800  
482 mm). It can be noticed also in this figure, that although the amount of irrigation given by the  
483 farmer was greater than the one simulated by the FAO model, the vegetation suffered from  
484 water stress during the summer (between DOY 228 and DOY 237). Such behaviour can be  
485 explained by inadequate distribution of irrigation: the wrong quantity is applied at the wrong  
486 moment. In fact, the farmer didn't apply the irrigation in this period while the model  
487 recommends the irrigation in the same period. It can be seen also that the farmer applied a  
488 large amount relatively to the required quantity given by the model. This is due to some  
489 unnecessary irrigation events during the rainfall period (e.g. DOY 169). The results revealed  
490 that the method of irrigation applied by the farmer was not appropriate for the olive orchards  
491 in the Tensift plain.

492 As we found above that an important amount of water ( $\approx 35\%$ ) was lost by direct soil  
493 evaporation during the wetting event, it is of interest to quantify the amount of water needed

494 to fulfill this water depleted from the topsoil layer ( $Z_e$ ). A similar parameter to  $K_s$  named soil  
495 evaporation reduction coefficient ( $K_r$ ) was deployed to schedule irrigation in the topsoil layer  
496 (Allen et al., 1998). Similarly to  $K_s$ , the estimation of  $K_r$  requires a daily water balance  
497 computation but for the surface soil evaporation layer  $Z_e$ . Figure 6b presents the evolution of  
498  $K_r$  with the timing and the amount of irrigation required. According to this figure,  $K_r$  varied  
499 between 0 and 1 depending to the amount of water available in the topsoil. Following heavy  
500 rainfall or irrigation, the evolution of  $K_r$  or soil evaporation rates can be described as two-  
501 stage process: an energy limiting stage, and a falling rate stage. In the first stage, the soil  
502 surface remains wet, the amount of water depleted by evaporation is equal to 0 and  $K_r$  is equal  
503 to 1. When the water content was reduced due to the depletion of water by evaporation  
504 (second stage) with the absence of rainfall and irrigation,  $K_r$  decreases and reaches 0 when the  
505 total evaporable water (TEW) was totally depleted. In this second stage, the soil evaporation  
506 rate decreases depending to the amount of water remaining in the surface soil layer and the  
507 soil hydraulic properties that determine the transfer of liquid and vaporized water to the  
508 surface. Ritchie (1972) funded that in the second stage the evaporation rate decreases as a  
509 function of the square root of time after wetting event. Based on the calculation of  $K_r$  by using  
510 the water balance equation (equations 74 and 77 in FAO 56), the timing and the amount of  
511 irrigations needed in the topsoil layer can be planned (Figure 6b) in order to compensate the  
512 water depleted from the topsoil layer ( $Z_e$ ). According to this figure, the irrigation is required  
513 by FAO when the soil water depletion is higher than the readily evaporable water ( $REW$ ) and  
514 no irrigation otherwise. The average value of irrigation recommended by FAO model in each  
515 supply was about 9 mm which corresponds to the value of  $REW$  except in the beginning of the  
516 calculation where it would be assumed as the total evaporable water (TEW=33.55 mm). The  
517 total amount of irrigation recommended by the FAO model for maintaining soil wet was about  
518 186 mm, which presents about 45% of the irrigation needed (411 mm) for avoiding olive

519 water stress. The cumulated values of total irrigation in the topsoil and in the root zone are  
520 about 597 mm for the simulated irrigation requirement by the FAO model and 800 mm for  
521 that given by the farmer, with a difference of 25%. This difference may be related to the  
522 inadequate amount and planning of irrigation by the farmer. Water amounts and timing are  
523 planned only by the understanding and perception of the farmer without using any guideline  
524 for scheduling the amount and timing of irrigation water applications. **Consequently, some**  
525 **irrigations are missing or unnecessary. For example on DOY 201 (July, 19), the model**  
526 **recommends the irrigation while the farmer didn't apply it in this day. Effectively, in this**  
527 **period, the irrigation is needed because the climatic demand was very higher in the summer.**  
528 **During the rainfall period (e.g. DOY 169), the irrigation is not necessary, but the farmer apply**  
529 **one. The results revealed that the method of irrigation applied by the farmer was not**  
530 **appropriate for the olive orchards in the Tensift plain.** It would be advisable to improve the  
531 irrigation management and to recommend the farmer to use the simple FAO model, which can  
532 be considered as a potentially useful tool for planning irrigation schedules on an operational  
533 basis.

## 534 **5. Conclusions**

535 The main objective of this study was to investigate the potential of the FAO-56 dual  
536 crop coefficient approach to provide accurate estimates of actual evapotranspiration (AET)  
537 and its components of the olive orchard in semi-arid region. Model simulations of evaporation  
538 and transpiration were compared to data obtained from a combination of eddy covariance  
539 based AET measurements and scaled-up sap flow measurements of transpiration.

540 The results showed that, by using the local values of basal crop coefficients derived  
541 from sap flow measurements, the approach simulates reasonably well AET over two growing  
542 seasons. The Root Mean Square Error (RMSE) between measured and simulated AET values  
543 during 2003 and 2004 were respectively about 0.54 and 0.71 mm per day. The value of basal



544 crop coefficient for the olive orchard used in this study was about 0.54. This value was lower  
545 than that suggested by the FAO-56 (0.62).

546 Since the FAO-56 dual crop coefficient approach predicts separately soil evaporation  
547 and plant transpiration, an attempt of comparison of the simulated components of  
548 evapotranspiration (soil evaporation and plant transpiration) with the measurements showed  
549 that the model gives an acceptable estimate of plant transpiration and soil evaporation. The  
550 RMSE between measured and simulated transpiration and soil evaporation (resp) were 0.59  
551 and 0.73 mm per day. In conclusion, it can be stated that the FAO-56 dual crop coefficient  
552 gives an encouraging result for partitioning of evaporation and transpiration despite the  
553 simplicity of the formulation used to derive such partition. Further effort will be necessary if  
554 more accurate simulation of ET partitioning is needed by this approach. This can be achieved  
555 by subdividing the plant transpiration into olive transpiration and understory transpiration and  
556 so two water balance are necessary for calculation stress coefficient  $K_s$ .

557 Additionally, the results of this study revealed that the irrigation scheme used by the  
558 farmer was not appropriate for the olive orchards in the Tensift plain. It was found that  
559 although the amount of irrigation applied by the farmer (800 mm) during the growing season  
560 of olive orchards was greater than the simulated one by the FAO model (411 mm), the  
561 vegetation suffered from water stress especially during the summer. Such behaviour can be  
562 explained by inadequate distribution of irrigation. It would be advisable to improve the  
563 irrigation management and to recommend the farmer to use the simple and operational FAO  
564 model for planning irrigation schedules.

## 565 **6. Acknowledgements**

566 This study was supported by SUDMED (IRD-UCAM) and PLEADeS projects funded  
567 by the European Union (PCRD). The authors are grateful to ORMVAH (*'Office Regional de*  
568 *Mise en Valeur Agricole du Haouz'*, Marrakech, Morocco) for its technical help. We thank the

569 director and staff of the Agdal olive orchard for access and use of the field site and for  
570 assistance with irrigation scheduling and security.

## 571 **7. Appendix**

572 Three statistics were used for analyzing the data: 1) the Mean Bias Error (MBE),  
573 which indicates the average deviation of the predicted values from the measured values; 2) the  
574 Root Mean Square Error (RMSE), which measures the discrepancy of predicted values around  
575 observed values; 3) the efficiency (E), which judges the performances of simulation data.

$$576 \quad MBE = \bar{y}_{mod} - \bar{y}_{obs}$$

$$577 \quad RMSE = \sqrt{\frac{1}{n} \sum_{i=1}^n (y_{i\ mod} - y_{i\ obs})^2}$$

$$578 \quad E = 1 - \frac{\sum_{i=1}^n (y_{i\ mod} - y_{i\ obs})^2}{\sum_{i=1}^n (y_{i\ obs} - \bar{y}_{obs})^2}$$

579 Where  $\bar{y}_{mod}$  and  $\bar{y}_{obs}$  are the averages of simulations and observations,  $n$  is the number of  
580 available observations,  $y_{i\ mod}$  and  $y_{i\ obs}$  are daily values of modeled and observed variables  
581 respectively.

582

## 583 **8. References**

584 [Abid Karray, J., Lhomme, J.P., Masmoudi, M.M., Ben Mechlia, N. 2008. Water balance of](#)  
585 [the olive tree–annual crop association: A modeling approach. Agric. Water Manage. 95, 575-](#)  
586 [586.](#)

587 Allen, R.G. 1996. Assessing integrity of weather data for use in reference evapotranspiration  
588 estimation. *J. Irrig. Drain Eng.* ASCE 122 (2), 97-106.

589 Allen, R.G., Pereira, L.S., Raes, D., Smith, M. 1998. Crop Evapotranspiration—Guidelines  
590 for Computing Crop Water Requirements, Irrigation and Drain, Paper No. 56. FAO, Rome,  
591 Italy, 300 pp.

592 Allen, R.G. 1999. Concept paper—accuracy of predictions of project-wide evapotranspiration  
593 using crop coefficients and reference evapotranspiration in a large irrigation project. In:  
594 Proceedings of the United States Committee on Irrigation and Drainage Conference on  
595 “Benchmarking Irrigation System Performance Using Water Measurement and Water  
596 Balances”, San Luis Obispo, CA, 10–13 March 1999.

597 Allen R.G. 2000. Using the FAO-56 dual crop coefficient method over an irrigated region as  
598 part of an evapotranspiration intercomparison study. *J. Hydrol.* 229, 27–41.

599 Allen, R.G., Pereira, L.S., Smith, M., Raes, D, and Wright, J.L. 2005a. FAO-56 dual crop  
600 coefficient method for estimating evaporation from soil and application extensions. *J. Irrig.*  
601 *Drain Eng.* ASCE 131 (1), 2-13.

602 Allen, R.G., Clemmens, A.J., Burt, C.M., Solomon, K, and O’Halloran, T. 2005b. Prediction  
603 accuracy for project-wide evapotranspiration using crop coefficient and reference  
604 evapotranspiration. *J. Irrig. Drain Eng.* ASCE 131 (1), 24-36.

605 Baldocchi, D.D., Law, B.E., Anthoni, P.M. 2000. On measuring and modeling energy fluxes  
606 above the floor of a homogeneous and heterogeneous conifer forest. *Agric. For. Meteorol.*  
607 102, 187–206.

608 Boulet, G., Chehbouni, A., Braud, I., Vauclin, M., Haverkamp, R., Zammit, C. 2000. A  
609 simple water and energy balance model designed for regionalization and remote sensing data  
610 utilization. *Agric. For. Meteorol.* 105, 117–132.

611 Braud, I., Dantas-Antonino, A.C., Vauclin, M., Thony, J.L., Ruelle, P. 1995. A simple soil-  
612 plant-atmosphere transfer model (SiSPAT) development and field verification. *J. Hydrol.* 166,  
613 213–250.

614 Brisson N., Mary B., Ripoche D et al. 1998. STICS: a generic model for the simulation of  
615 crops and their water and nitrogen balances. I. Theory and parametrization applied to wheat  
616 and corn. *Agron. J.* 18, 311-346.

617 Burgess S.S.O., M.A. Adams, N.C. Turner, and C.K. Ong. 1998. The redistribution of soil  
618 water by tree root systems. *Oecologia.* 115, 306-311.

619 Burgess, S.S.O., Adams, M.A., Turner, N.C., Beverly, C.R., Ong, C.K., Khan, A.A.H., Bleby,  
620 T.M. 2001. An improved heat pulse method to measure slow and reverse flow in woody  
621 plants. *Tree Physiol.* 21, 589-598

622 Chehbouni, A., Escadafal, R., Duchemin, B., Boulet, G., Simonneaux, V., Dedieu, G.,  
623 Mougnot, B., Khabba, S., Kharrou, H., Maisongrande, P., Merlin, O., Chaponnière, A.,  
624 Ezzahar, J., Er-Raki, S., Hoedjes, J., Hadria, R., Abourida, A., Cheggour, A., Raibi, F., A.  
625 Boudhar, A., Benhadj, I., Hanich, L., Benkaddour, A., Guemouria, N., Chehbouni, Ah.,  
626 Lahrouni, A., Oliosio, A., Jacob, F., Williams, D. G., Sobrino, J. 2008. An integrated  
627 modelling and remote sensing approach for hydrological study in arid and semi-arid regions:  
628 the SUDMED Programme. *Int. J. Remote Sens.*, 29, 17 & 18, 5161 – 5181.

629 Duchemin, B., Hadria, R., Er-Raki S., Boulet, G., Maisongrande, P., Chehbouni, A.,  
630 Escadafal, R., Ezzahar, J., Hoedjes, J., Karrou, H., Khabba, S., Mougnot, B., Oliosio, A.,  
631 Rodriguez, J-C., Simonneaux, V. 2006. Monitoring wheat phenology and irrigation in Central  
632 Morocco: on the use of relationship between evapotranspiration, crops coefficients, leaf area  
633 index and remotely-sensed vegetation indices. *Agric. Water Manage.* 79, 1- 27.

634 Eitzinger J., Marinkovic D., Hösch J. 2002. Sensitivity of different evapotranspiration  
635 calculation methods in different crop-weather models. In Rizzoli, A.E., Jakeman, A.J. (Eds.):

636 Integrated Assessment and Decision Support; Proc., 1st biennial meeting of the International  
637 Environmental Modelling and Software Society (IEMSS), 24-27 June 2002, Lugano,  
638 Switzerland. 2, 395-400.

639 Er-Raki, S., Chehbouni, A., Guemouria, N., Duchemin, B., Ezzahar, J., Hadria, R., BenHadj,  
640 I. 2006. Driven FAO-56 dual crop coefficient approach with remotely-sensed data for  
641 estimating water consumptions of wheat crops in a semi-arid region. The 2nd International  
642 Symposium on Recent Advances in Quantitative Remote Sensing: RAQRS'II, 25-29  
643 September 2006, Valencia, Spain.

644 Er-Raki S., Chehbouni G., Guemouria, N., Duchemin B., Ezzahar J., Hadria R.  
645 2007. Combining FAO-56 model and ground-based remote sensing to estimate water  
646 consumptions of wheat crops in a semi-arid region. *Agric. Water Manage.* 87, 41–54.

647 Er-Raki, S., Chehbouni, A., Hoedjes, J., Ezzahar, J., Duchemin, B., Jacob, F. 2008.  
648 Improvement of FAO-56 method for olive orchards through sequential assimilation of  
649 Thermal infrared based estimates of ET. *Agric. Water Manage.* 95, 309–321.

650 Er-Raki, S., Chehbouni, A., Guemouria, N., Ezzahar, J., Khabba, S., Boulet, G. and Hanich,  
651 L. 2009. Citrus orchard evapotranspiration: Comparison between eddy covariance  
652 measurements and the FAO 56 approach estimates. *Plant Biosys.* 143 (1), 201-208.

653 Er-Raki, S., Chehbouni, A., Duchemin, B. 2010. Combining satellite remote sensing data with  
654 the FAO-56 dual approach for water use mapping in irrigated wheat fields of a semi-arid  
655 region. *Remote Sens.* 2(1), 375-387.

656 Evett, S.R., Howell, T.A., Schneider, A.D., Tolk, J.A. 1995. Crop Coefficient Based  
657 Evapotranspiration Estimates Compared with Mechanistic Model Results. In W.H. Espey, and  
658 P.G. Combs (ed.). *Water resources engineering*, vol. 2, Proc. of the First International  
659 Conference, Aug. 14-18 1995, San Antonio (Texas, USA).

660 Ezzahar J., Chehbouni, A., Hoedjes, J.C.B., Er-Raki, S., Chehbouni, Ah., Bonnefond, J-M.  
661 and De Bruin, H.A.R. 2007. The use of the Scintillation Technique for estimating and  
662 monitoring water consumption of olive orchards in a semi-arid region. *Agric. Water Manage.*  
663 89, 173-184.

664 Fernández, J.E., Moreno, F., 1999. Water use by the olive tree. *Journal of Crop Production.* 2  
665 (2), 101–162.

666 Fernández, J. E., M. J. Palomo, A. Díaz-Espejo et al. 2001. Heat-pulse measurements of sap  
667 flow in olives for automating irrigation: tests, root flow and diagnostics of water stress. *Agric.*  
668 *Water Manage.* 51, 99-123.

669 Ford, C. R., Hubbard, R.M., Kloeppe, B. D, Vose, J. M. 2007. A comparison of sap flux-  
670 based evapotranspiration estimates with catchment-scale water balance. *Agric. For. Meteorol.*  
671 145, 176–185.

672 Gómez, J. A., Giráldez, J. V. and Fereres E. 2001. Rainfall interception by olive trees in  
673 relation to leaf area. *Agric. Water Manage.* 49(1), 56-78.

674 González-Dugo, M.P., Mateos, L. 2008. Spectral vegetation indices for benchmarking water  
675 productivity of irrigated cotton and sugarbeet crops. *Agric. Water Manage.* 95(1), 48-58.

676 Hoedjes, J.C.B., Chehbouni, A., Ezzahar, J., Escadafal, R., De Bruin, H.A.R., 2007.  
677 Comparison of large aperture scintillometer and eddy covariance measurements: can thermal  
678 infrared data be used to capture footprint induced differences? *J. Hydrometeorol.* 8 (2), 144-  
679 159.

680 Hunsaker, DJ., Pinter, PJ Jr., Barnes, EM., Kimball, BA. 2003. Estimating cotton  
681 evapotranspiration crop coefficients with a multispectral vegetation index. *Irrig. Sci.* 22, 95-  
682 104.

683 Hunsaker, DJ., Pinter, PJ Jr., Kimball, BA. 2005. Wheat basal crop coefficients determined  
684 by normalized difference vegetation index. *Irrig. Sci.* 24, 1-14.

685 Huxman, T.E., Wilcox, B.P., Breshears, D.D., Scott, R.L., Snyder, K.A., Small, E.E., Hultine,  
686 K., Pockman, W.T., Jackson, R.B. 2005. Ecohydrological implications of woody plant  
687 encroachment. *Ecology*. 86, 308–319.

688 Itenfisu, D. 1998. Adaptation of resistance-based evapotranspiration functions to row crops.  
689 Unpublished PhD dissertation, Dept. Biol. and Irrig. Engng, Utah State Univ., Logan, UT,  
690 207pp.

691 Kite, G. W., Droogers P. 2000. Comparing evapotranspiration estimates from satellites,  
692 hydrological models and field data. *J. Hydrol.* 209, 3-18.

693 Kumagai, T., Nagasawa, H., Mabuchi, T., Ohsakia, S., Kubota, K., Kogia, K., Utsumi, Y.,  
694 Kogaa, S., Otsuki, K., 2005. Sources of error in estimating stand transpiration using allometric  
695 relationships between stem diameter and sapwood area for *Cryptomeria japonica* and  
696 *Chamaecyparis obtuse*. *Agric. For. Meteorol.* 206, 191–195.

697 Liu, Y., Luo, Y. 2010. A consolidated evaluation of the FAO-56 dual crop coefficient  
698 approach using the lysimeter data in the North China Plain. *Agric. Water Manage.* 97, 31-40.

699 Martinez-Cob, A., Faci, J.M. 2010. Evapotranspiration of an hedge-pruned olive orchard in a  
700 semiarid area of NE Spain. *Agric. Water Manage.* 97, 410-418.

701 Monteith, J. L. 1965. *Evaporation and Environment*. 19<sup>th</sup> Symposia of the Society for  
702 Experimental Biology, University Press, Cambridge, 19:205-234.

703 Moran, M.S., R.L. Scott, T.O. Keefer, W.E. Emmerich, M. Hernandez, G.S. Nearing, G.B.  
704 Paige, M.H. Cosh, P.E. O'Neill. 2009. Partitioning evapotranspiration in semiarid grassland  
705 and shrubland ecosystems using time series of soil surface temperature. *Agric. For. Meteorol.*  
706 149, 59-72.

707 Noilhan, J., Mahfouf, J.F. 1996. The ISBA land surface parameterisation scheme. *Global and*  
708 *Planetary Change*, 13:145-159.

709 Oishi, C.A., Oren, R., Stoy, P.C. 2008. Estimating components of forest evapotranspiration: A  
710 footprint approach for scaling sap flux measurements. *Agric. For. Meteorol*, 148, 1719-1732.

711 Olioso, A., Chauki, H., Courault, D., and Wigneron, J.-P. 1999. Estimation of  
712 evapotranspiration and photosynthesis by assimilation of remote sensing data into SVAT  
713 models. *Remote Sens. Environ.* 68, 341–356.

714 Paço, T. A., Ferreira, M. I., Conceição, N. 2006. Peach orchard evapotranspiration in a sandy  
715 soil: Comparison between eddy covariance measurements and estimates by the FAO 56  
716 approach. *Agric. Water Manage.* 85, 305-313.

717 Palomo, M.J., Moreno, F., Fernandez, J.E., Diaz- Espejo, A., Giron, I.F. 2002. Determining  
718 water consumption in olive orchards using the water balance approach. *Agric. Water Manage.*  
719 55, 15-35.

720 Peng, S., Ding, J., Mao, Z., Xu, Z., Li, D., 2007. Estimation and verification of crop  
721 coefficient for water saving irrigation of late rice using the FAO-56 method. *Transactions of*  
722 *the CSAE* 23 (7), 30–34.

723 Reynolds, JF, Kemp, PR, Tenhunen, JD. 2000. Effects of long-term rainfall variability on  
724 evapotranspiration and soil water distribution in the Chihuahuan Desert: a modeling analysis.  
725 *Plant Ecology.* 150, 145–159.

726 Ritchie, J.T., 1986. The CERES-Maize model In: *CERES-Maize: Simulation model of maize*  
727 *growth and development.* Ed by Jones C.A., and Kiniry J.R., Texas A M University press,  
728 college station, Tx., (1986) 3-6.

729 Ritchie, J.T. 1972. Model for predicting evaporation from a row crop with incomplete cover.  
730 *Water Resour. Res.* 8:1204-1213.

731 Scott, R.L., Huxman, T.E., Cable, W.L. and Emmerich, W.E. 2006. Partitioning of  
732 evapotranspiration and its relation to carbon dioxide exchange in a Chihuahuan desert  
733 shrubland. *Hydrol. Proces.* 20, 3227–3243.



734 Sinclair, T.R., and Seligman, N.G. 1996. Crop modeling: from infancy to maturity. *Agron. J.*  
735 88, 698-704.

736 Teixeira, A.H. de C., Bastiaanssen, W.G.M., Moura, M.S.B., Soares, J.M., Ahmad, M.D.,  
737 Bos, M.G. 2008. Energy and water balance measurements for water productivity analysis in  
738 irrigated mango trees, Northeast Brazil. *Agric. For. Meteorol.* 148, 1524-1537.

739 Testi, L., Villalobos, F.J., Orgaz, F. 2004. Evapotranspiration of a young irrigated olive  
740 orchard in southern Spain. *Agric. For. Meteorol.* 12, 1-18.

741 Twine, T.E., Kustas, W.P., Norman, J.M. et al. 2000. Correcting Eddy-Covariance Flux  
742 Underestimates over a Grassland. *Agric. For. Meteorol.* 103, 279-300.

743 Villalobos, F.J., Orgaz, F., Testi, L., Fereres, E. 2000. Measurements and modeling of  
744 evapotranspiration of olive (*Olea europaea* L.) orchards. *Eur. J. Agron.* 13, 155-163.

745 Williams, D.G., Cable, W., Hultine, K., Yepez, E.A., Er-Raki, S., Hoedjes, J.C.B., Boulet, G.,  
746 de Bruin, H.A.R., Chehbouni, A. et Timouk, F. 2003. Suivi de la répartition de  
747 l'évapotranspiration dans une oliveraie (*Olea europaea* L.) à l'aide des techniques de l'eddy  
748 covariance, des flux de sève et des isotopes stables ». *Vèmes Journées de l'Ecologie*  
749 *Fonctionnelle*, 12 au 14 Mars 2003 à Nancy.

750 Williams, D.G., Cable, W., Hultine, K., Hoedjes, J.C.B., Yepez, E.A., Simonneaux, V., Er-  
751 Raki, S., Boulet, G., de Bruin, H.A.R., Chehbouni, A., Hartogensis, O.K. and Timouk, F.  
752 2004. Evapotranspiration components determined by stable isotope, sap flow and eddy  
753 covariance techniques. *Agric. For. Meteorol.* 125, 241-258.

754 Yepez, E.A., Huxman, T.E., Ignace, D.D., English, N.B., Weltzin, J.F., Castellanos, A.E. and  
755 Williams, D.G. 2005. Transpiration and evaporation following a moisture pulse in semiarid  
756 grassland: a chamber-based isotope method for partitioning evapotranspiration. *Agri. For.*  
757 *Meteorol.* 132, 359–376.

758 Yunusa, I.A.M., Walker, R.R., Guy, J.R. 1997. Partitioning of seasonal evapotranspiration  
759 from a commercial furrow irrigated Sultana vineyard. *Irrig. Sci.* 18, 45–54.

760

761 **Figure captions**

762 **Figure 1.** Daily reference evapotranspiration  $ET_0$  calculated following the FAO-Penman-  
763 Monteith equation during 2003 (top) and 2004 (bottom) growing seasons. Rainfall and  
764 irrigation events are shown in the same figures.

765 **Figure 2.** Assessment of energy balance closure. Daily average fluxes of net radiation ( $R_n$ )  
766 minus the soil heat flux ( $G$ ) are compared against the sums of sensible ( $H_{EC}$ ) and latent heat  
767 ( $L_v E_{EC}$ ) measured by the eddy covariance system.

768 **Figure 3.** Daily evolution of the difference between the soil moisture at 5 cm depth on day  $i$   
769 and on day  $i-1$  ( $\Delta\theta$ ). The vertical dotted line shows the date on which the soil evaporation was  
770 negligible.

771 **Figure 4.** Time course of observed (triangles on dotted line) and simulated (solid line) actual  
772 evapotranspiration using the **FAO-56 dual crop coefficient approach** for 2003 (top) and 2004  
773 (bottom) growing seasons of olives orchard in Tensift Alhaouz, Marrakech Morocco.

774 **Figure 5.** Time course of observed (triangles on dotted line) and simulated (solid line) two  
775 components of evapotranspiration using the FAO-56 dual crop coefficient approach of olives  
776 orchard in Tensift Alhaouz, Marrakech Morocco during the 2004 growing season (from  
777 DOY130 to DOY272): a) plant transpiration, b) soil evaporation. The measured soil  
778 evaporation is computed as the difference between measured evapotranspiration by eddy  
779 covariance system and measured transpiration by sap flow. Note that the negative values of  
780 measured soil evaporation obtained when the measured transpiration is higher than measured  
781 ( $AET$ ) by eddy covariance system, were taken equal zero.

782 **Figure 6.** Estimated daily soil water stress coefficient  $K_s$  (figure a) and daily soil evaporation  
783 reduction coefficient  $K_r$  (figure b) by the FAO-56 dual crop coefficient approach for the olives  
784 orchard in Tensift Alhouz, Marrakech Morocco during 2004 growing season. Amount and

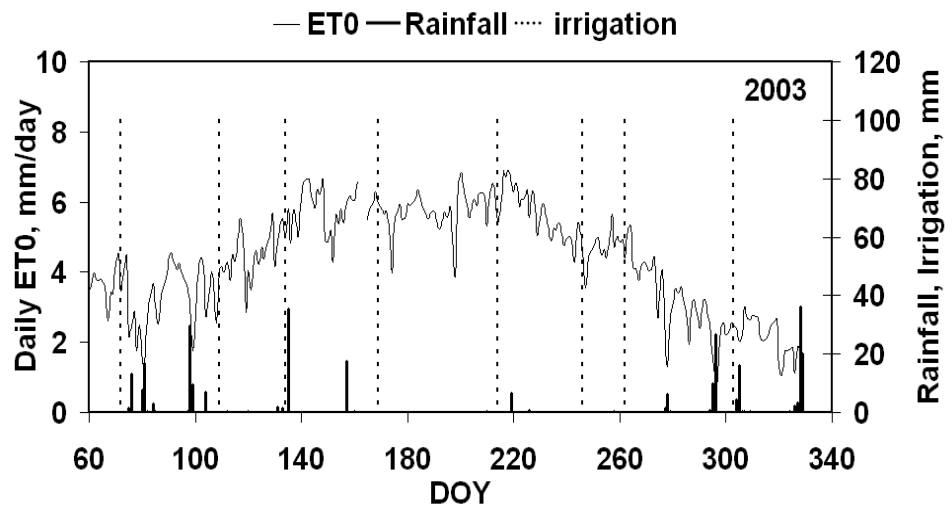
785 frequency of irrigation given by the farmer and recommended by the FAO model are shown  
786 in the same figures.

787

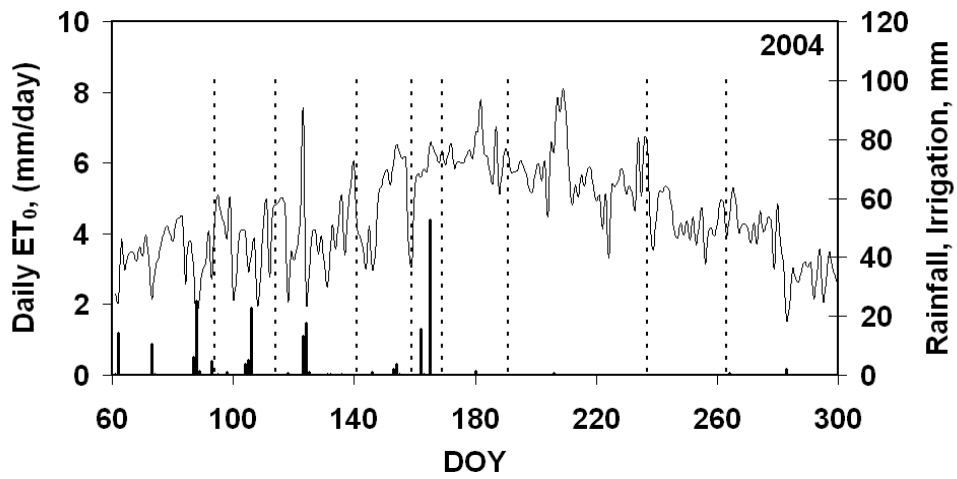
788

789  
790

Figure 1



791



792

793

794

795

796

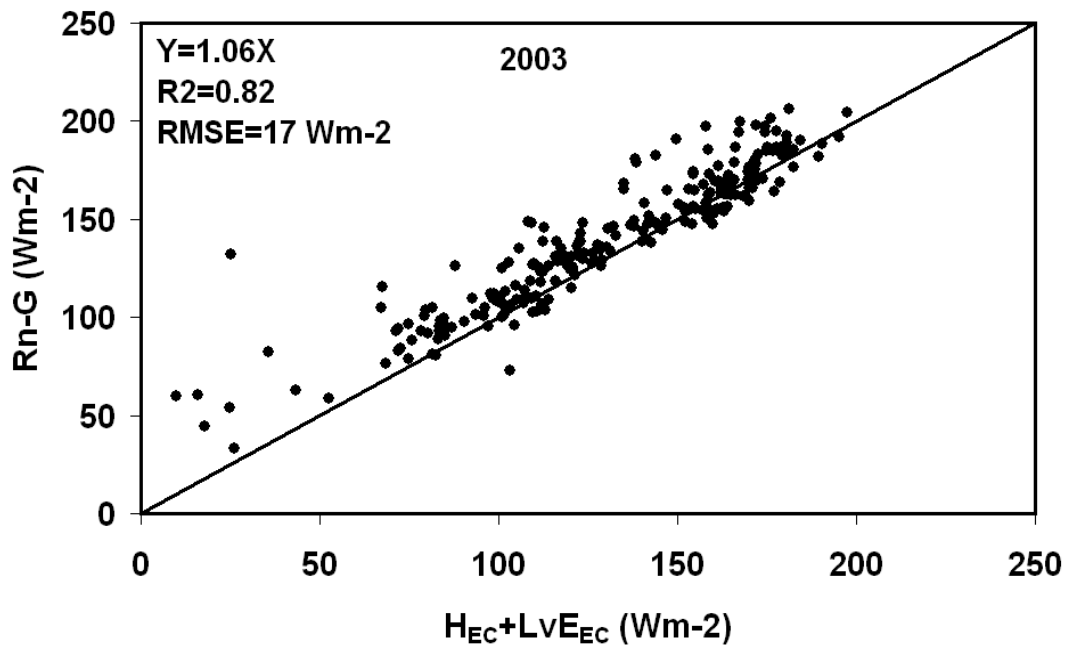
797

798

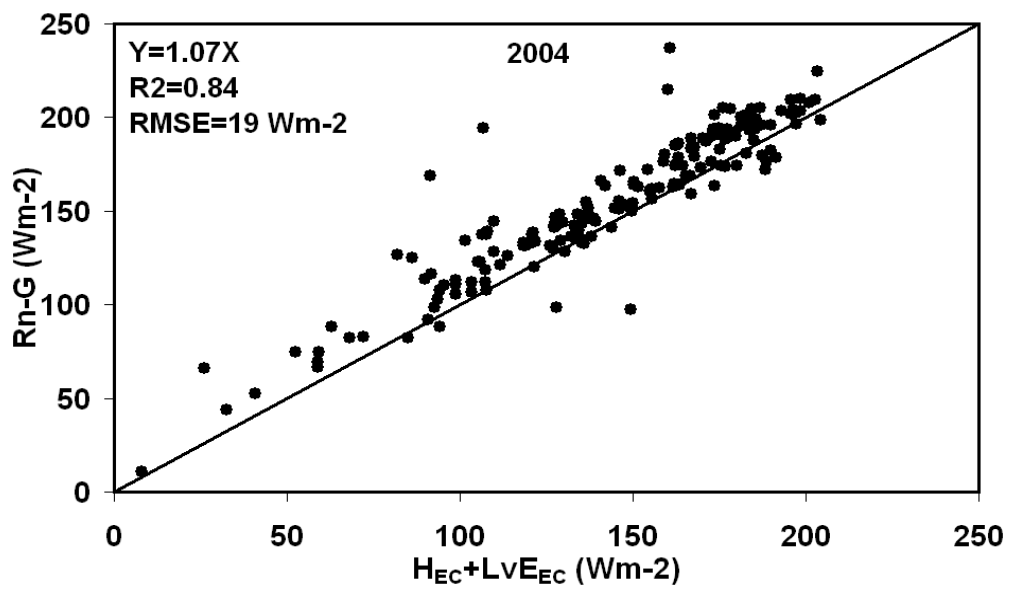
Figure 2

799

800



801



802

803

804

805

806

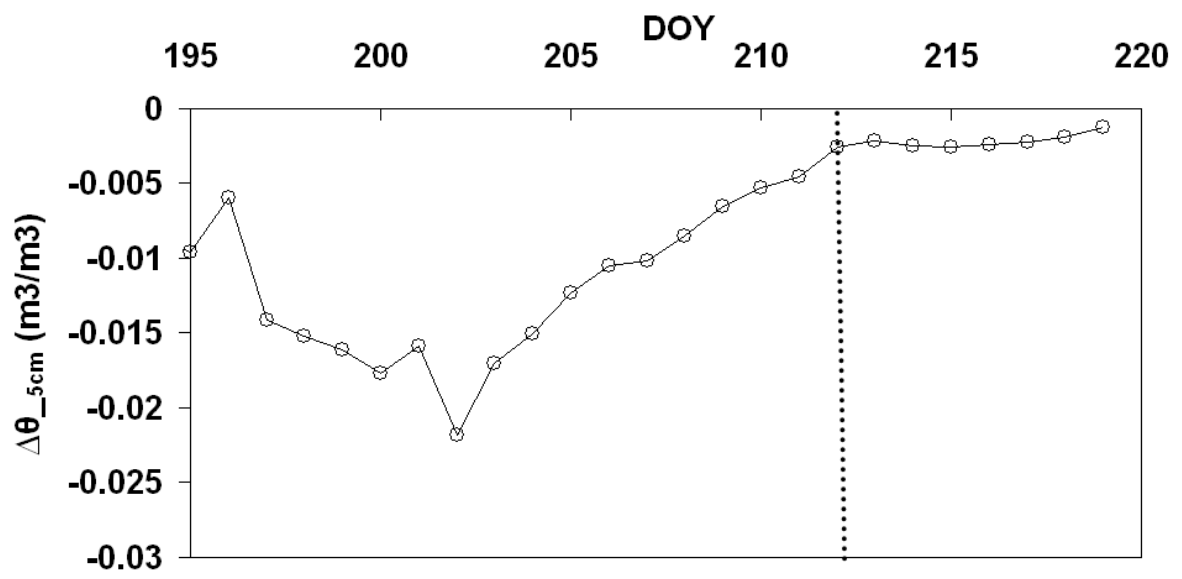
Figure 3

807

808

809

810



811

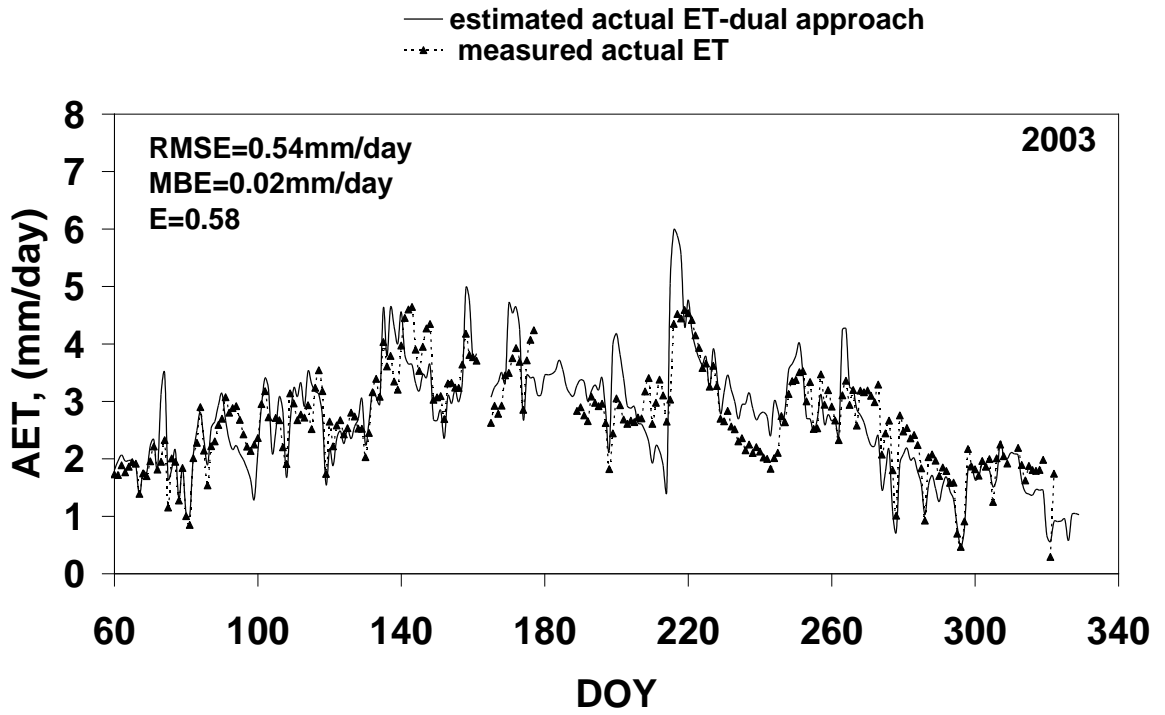
812

813

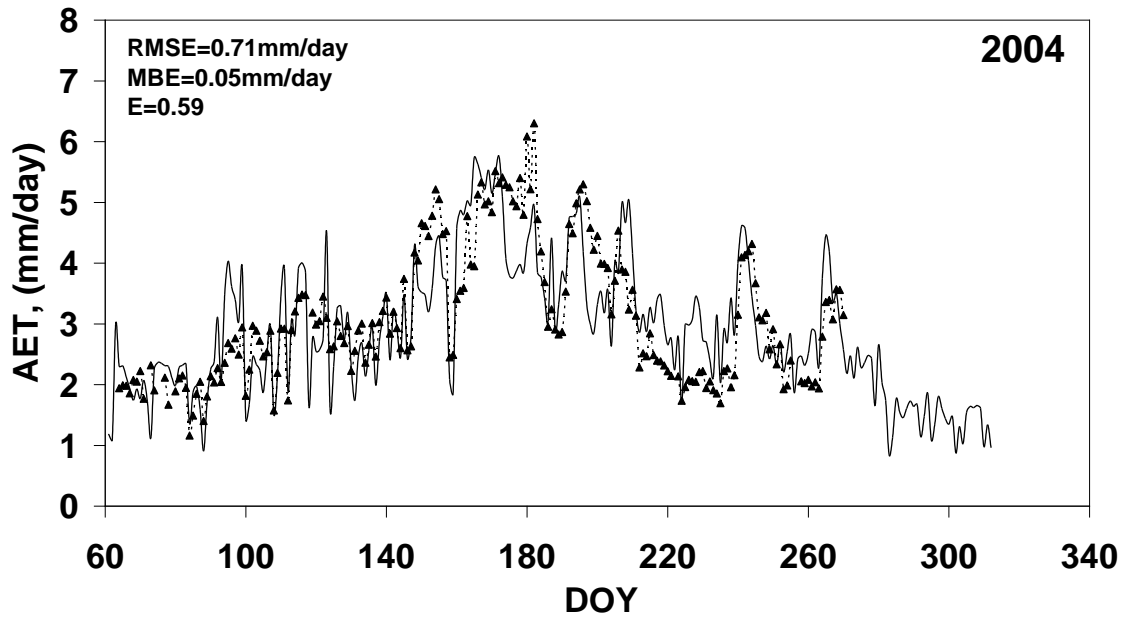
814

815  
816  
817

Figure 4



818

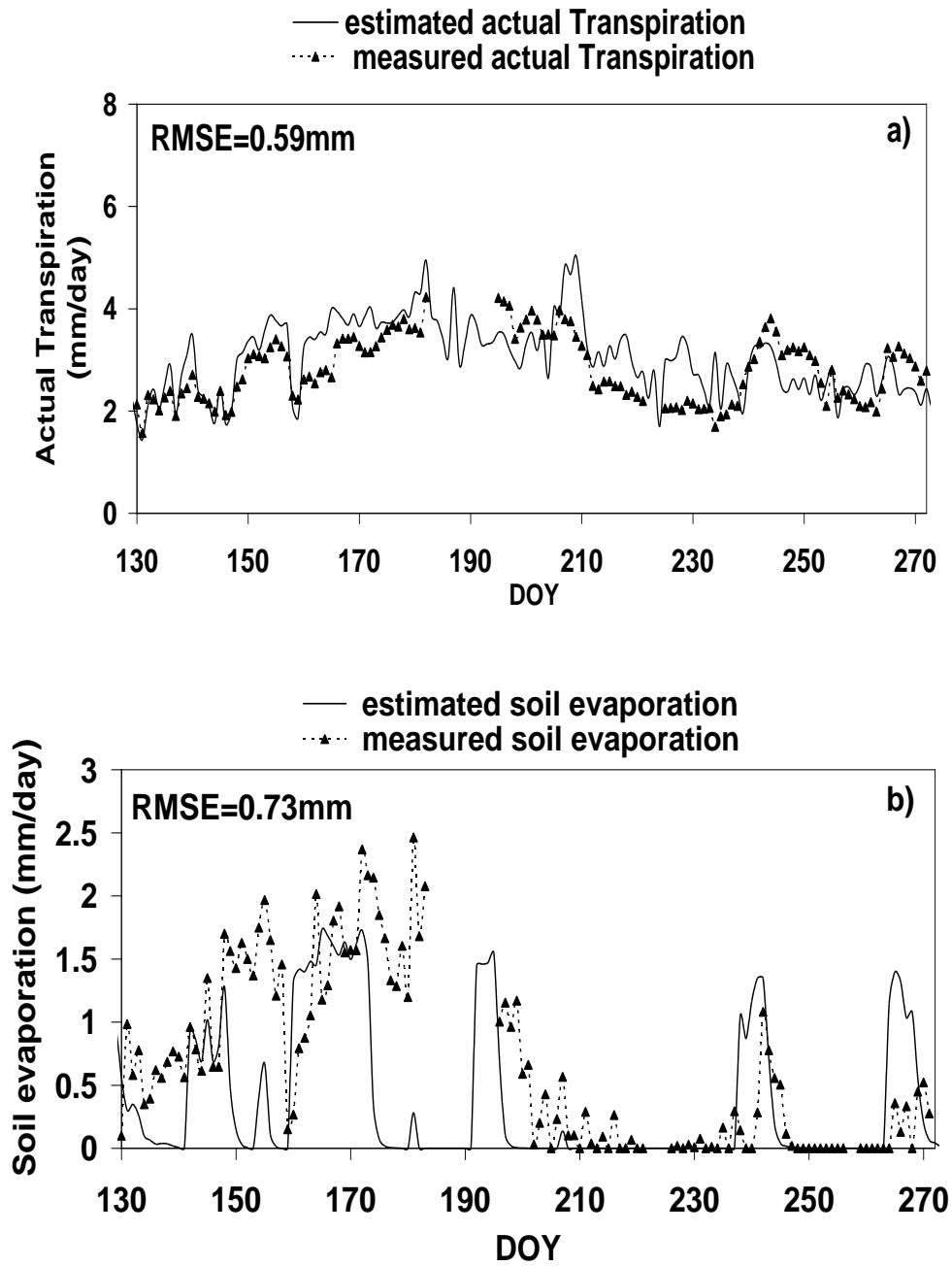


819  
820  
821



822  
823  
824

Figure 5



825

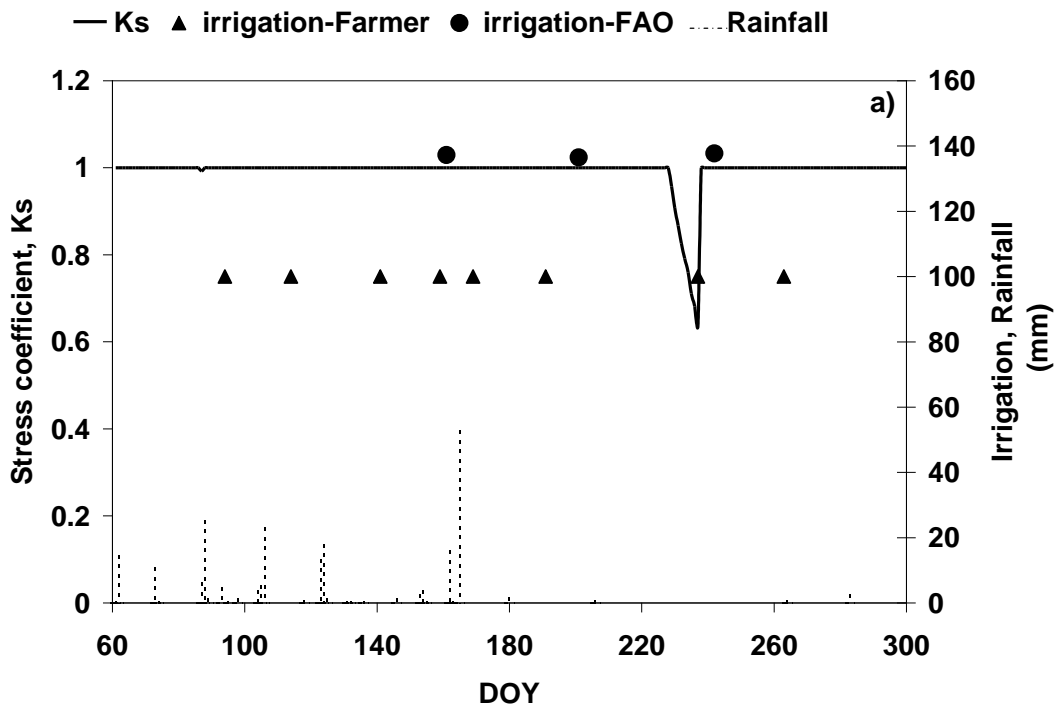
826

827

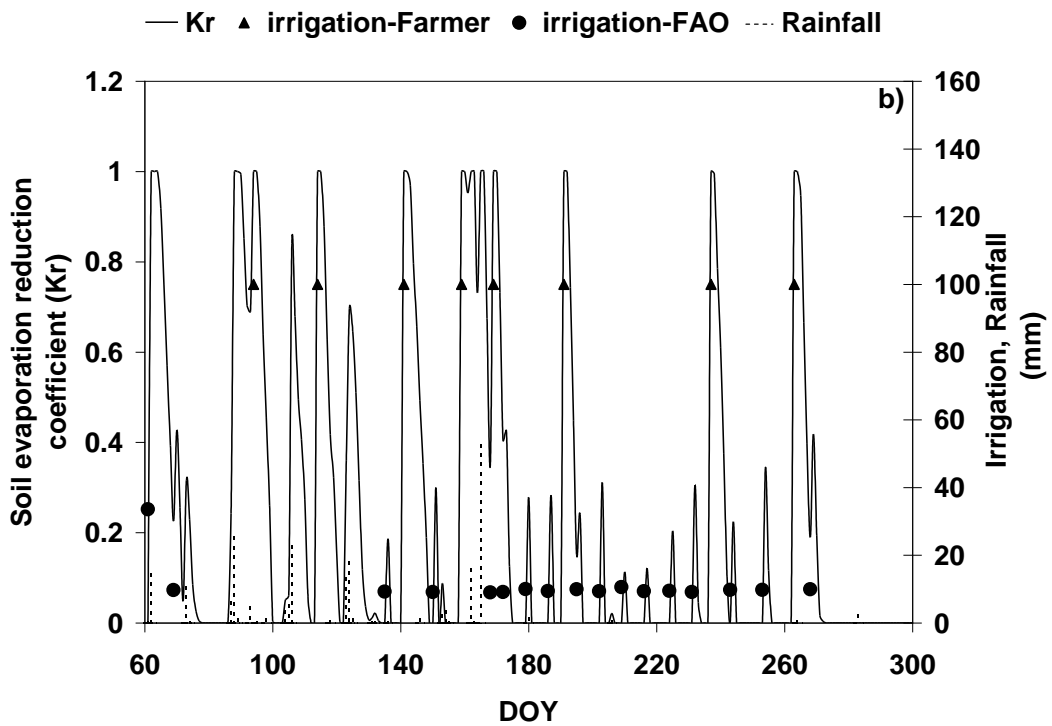
828

829  
830  
831

Figure 6



832  
833  
834



835  
836  
837  
838  
839